Sub-grid-scale Effects on Short-wave Instability in Magnetized Hall-MHD Plasma

H. Miura and N. Nakajima

National Institute for Fusion Science, 322-6 Oroshi, Toki, Gifu 509-5292, JAPAN

E-mail contact of main author:miura.hideaki@nifs.ac.jp

Abstract. Aiming to clarify effects of short-wave modes on nonlinear evolution/saturation of the ballooning instability in the Large Helical Device, fully three-dimensional simulations of the single-fluid MHD and the Hall MHD equations are carried out. A moderate parallel heat conductivity plays an important role both in the two kinds of simulations. In the single-fluid MHD simulations, the parallel heat conduction effectively suppresses short-wave ballooning modes but it turns out that the suppression is insufficient in comparison to an experimental result. In the Hall MHD simulations, the parallel heat conduction triggers a rapid growth of the parallel flow and enhance nonlinear couplings. A comparison between single-fluid and the Hall MHD simulations reveals that the Hall MHD model does not necessarily improve the saturated pressure profile, and that we may need a further extension of the model. We also find by a comparison between two Hall MHD simulations with different numerical resolutions that sub-grid-scales of the Hall term should be modeled to mimic an inverse energy transfer in the wave number space.

1 Introduction

A magnetohydrodynamics (MHD) instability has been one of the most important subjects to understand hot plasma dynamics in a torus device. An aspect of MHD instability of the Large Helical Device, LHD[1, 2], can be characterized by the position of the vacuum magnetic axis R_{ax}. The standard position of the axis is $R_{ax} = 3.75m$. When R_{ax} is shorter than $3.75m$, we call its magnetic configuration *inwardly shifted*. On one hand, the pressure-driven instabilities such as the interchange instability and the ballooning instability are considered to be a key factor of the beta-limit in operations. Such an unstable nature is stronger for a shorter R_{ax}. On the other hand, an experimental fact is that high-beta values have been achieved under inwardly shifted magnetic configurations[3, 4, 5]. For the purpose of understanding how the hot plasma could overcome the dangerous instabilities, nonlinear evolutions of the pressure-driven instabilities have been studied numerically[6, 7, 8, 9]. An understanding is that some nonlinear processes such as the pressure profile modification help a mild saturation of the instability. It has also been pointed out that the compressibility effect, generation of flows parallel to the magnetic field lines and the parallel heat conduction can contribute to the saturation significantly[8, 10, 11].

Although some insights are given by the numerical works, we have not reached to a conclusive understanding on some aspects of the saturation of the pressure-driven instability yet. For example, an importance of the short-wave pressure-driven modes on the mild saturation still remains unclear. While the pressure-driven modes have a property that their growth rates are larger for shorter wavelength, we are not able to resolve infinitely short wavelength in a numerical simulation and need to truncate/damp scales shorter than its numerical resolution. A physical justification of the artificial truncation was that a local flattening of the pressure profile, caused by the nonlinear coupling of unstable modes, could suppress growth of other unstable modes. However, our recent simulations have revealed that it could not suppress at least when the ballooning modes grow in a very unstable profile[11]. A physical dissipation can damp the small scales but the dissipative

length scale in the direction perpendicular to the magnetic field lines is usually quite shorter than a numerical resolution. Another possibility is that the growth of the short-wave unstable modes are suppressed by a sort of a parallel dissipation such as the parallel heat conduction, and we do not need an infinite resolution to resolve them. We have reported that the parallel heat conduction works quite effectively, and the moderate and high wave number ballooning modes are suppressed even when the initial equilibrium is very unstable[11]. However, it is also reported that the suppression of the growth is not sufficient even with the help of the parallel heat conduction, and we need further survey on this subject.

The purpose of this article is twofold. The first one is to report a recent progress on the numerical study of the nonlinear evolution of the ballooning modes. The second one is to obtain some basic information to construct sub-grid-scale models of the equations. This is motivated to compromise a time-consuming nature of a three-dimensional (3D) extended MHD simulation associated with fast waves of two-fluid systems and increasing requirements for quick numerical experiments by so-called large eddy simulations of extended MHD models.

This paper is organized as follows. In §2, the initial equilibrium which is used as the initial condition of our simulations is shown. In §3, numerical results of our recent MHD simulations are shown. In §4, numerical results of the Hall MHD simulations are shown. In §5, sub-grid-scale effects of the Hall term is studied, referring to some numerical results of the Hall MHD turbulence. The concluding remarks are in §6.

2 Initial equilibrium and linear stability

We solve fully 3D single-fluid MHD/Hall MHD equations by the use of the MHD In Non-Orthogonal System (MINOS) code[8, 9, 11]. The equations have four dissipative coefficients, the resistivity η, the perpendicular heat conductivity $\kappa_\perp$, the parallel heat conductivity $\kappa_\parallel$, and the viscosity μ. In addition to the dissipative coefficients, the Hall parameter ε controls the ion skin depth. By setting $\varepsilon = 0$, the single-fluid MHD equations are recovered. See Refs.[8, 9, 11] for the details of the normalization of the MHD equations, numerical techniques and parameters. All of our 3D simulations are carried out for the inwardly shifted LHD configuration of the magnetic axis position $R_{ax} = 3.6m$. The initial equilibrium is computed by the use of the HINT code[12]. This equilibrium has a peaked pressure profile $p(\psi) \simeq P_0(1-\psi)^2$ and the uniform mass density $\rho(\psi) = 1$. The peak beta value at the magnetic axis $\beta_0 \equiv P_0/(B_0^2/2)$ is 3.7%, and the averaged beta value is $\langle\beta\rangle \simeq 1.2\%$ where $\langle\ \rangle$ is the volume average over the finite-β region, over which we construct the Boozer coordinate later. In Fig.1, the peak beta value β_0, the rotational transform $\iota/2\pi$ and the Mercier index D_I with positive value (multiplied by $1/20$) are plotted as the function of the normalized minor radius $\sqrt{\psi}$. The value $D_I \simeq 0.4$ in Fig.1 indicates that the equilibrium is fairly unstable according to the linear analysis[4]. This initial equilibrium has been used as the initial condition of 3D simulations in Ref.[11]. Readers refer to the reference for details of the initial equilibrium and its linear stability properties. In the reference, the unstable modes which grow from the initial equilibrium are identified as the ballooning modes.

In this article we provide two sets of grid points (H)$193 \times 193 \times 640$ and (L)$97 \times 97 \times 640$ for the same initial equilibrium. We construct the Boozer coordinates (ψ, θ, ζ), where ψ, θ and ζ are the toroidal flux divided by 2π, the poloidal and the toroidal angles, respectively, so that we can project a physical quantity $A(\boldsymbol{x})$ on the Boozer coordinate as $A(\psi, \theta, \zeta)$ and compute its Fourier coefficients. A Fourier coefficient of $A(\boldsymbol{x})$ is denoted as $A_{mn}(\psi)$, where m and n are the poloidal and toroidal wave numbers, respectively. A 3D vector field $\boldsymbol{V}$ is decomposed into the three components, normal, parallel and binormal for the three orthogonal directions $\boldsymbol{e}_{\nabla\psi} = \nabla\psi/|\nabla\psi|$, $\boldsymbol{e}_b = \boldsymbol{B}/|\boldsymbol{B}|$, and $\boldsymbol{e}_{\nabla\psi\times b} = \boldsymbol{e}_{\nabla\psi} \times \boldsymbol{e}_b$, respectively, where $\boldsymbol{B}$ is the magnetic field vector. Then we

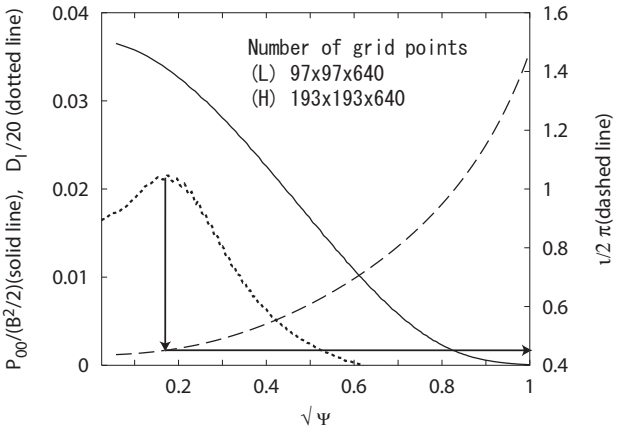

FIG. 1: Radial profiles of the pressure P_{00}, the rotational transform $\iota/2\pi$ and the Mercier index D_I of the initial equilibrium are plotted. In order for later use, the two resolutions $97\times97\times640$ and $193\times193\times640$, are provided.

transform the three components to the Fourier coefficients.

3 MHD simulations

Our recent MHD simulations ($\varepsilon = 0$) show that a moderate parallel heat conductivity $\kappa_\parallel = 1\times10^{-2}$ helps the saturation of the ballooning modes through both linear and nonlinear stages in comparison to a simulation with a small parallel heat conductivity $\kappa_\parallel = 1\times10^{-6}$[11]. In Fig.2, the mean pressure profiles $P_{00}(\sqrt{\psi})$ of the two simulations with different values of $\kappa_\parallel$, 1×10^{-2} and 1×10^{-6}, are shown. When the moderate value $\kappa_\parallel = 1\times10^{-2}$ is adopted, the generation of the flow

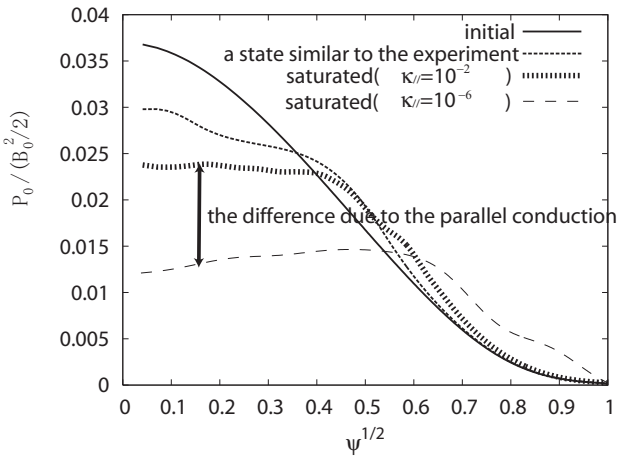

FIG. 2: A comparison of the mean pressure profiles $P_{00}(\sqrt{\psi})$ between simulations with and without $\kappa_\parallel$.

parallel to the magnetic field lines is enhanced because of the lack of the parallel pressure gradient $\nabla_\parallel P$. Consequently, the parallel heat conduction works not only to reduce the linear growth rates of the ballooning modes but also to release the free energy into the parallel kinetic energy and help a mild saturation. We find in Fig.2 that the saturated P_{00} profile in the simulation of $\kappa_\parallel = 1\times10^{-2}$ is much better than that of the other one.

Although the simulation with the moderate $\kappa_\parallel$ provides a relatively mild saturation, it does not coincide with an experimental result satisfactory. For example, a pressure profile P_{00} observed in the course of the time evolution in Fig.2 ('*a state similar to the experiment*', in a thin dashed line) is similar to that reported by Sakakibara et al.[13], because of the local flattening of the profile at $\sqrt{\psi} \simeq 0.3$ where the $\iota/2\pi = 0.5$ rational surface exists. In the experimental report, the beta value was limited when the $\iota/2\pi = 0.5$ rational surface was observed, and was raised when the rational surface disappeared. We consider that the limited profile in the experiment can be the counterpart of the saturated profile of our numerical simulation. However, in the MHD simulation ($\kappa_\parallel = 1 \times 10^{-2}$, the deformation is not terminated in *a state similar to the experiment* but is continued until the saturated profile of thick dotted line in Fig.2. It suggests that we need further stabilizing effects other than the parallel heat conduction. However, so far, we do not find a sufficient stabilization mechanism for the unstable equilibrium profile in the framework of the classical single-fluid MHD model. (Off course we could stabilize the instability by raising the perpendicular heat conductivity, $\kappa_\perp = 10^{-4}$ for example. However, we consider that such a large $\kappa_\perp$ cannot be justified within the single-fluid MHD model and need an extended model.) A possible candidate of the stabilizing effects might be found in some two-fluid effects. For example, Huba[14] reported that the moderate wave number Rayleigh-Taylor instability could be suppressed by the Hall effect. It motivates us to carry out simulations of an extended model in order to clarify how a coincidence between the experimental and numerical results can be obtained.

4 Hall MHD simulations

Here we study the Hall MHD dynamics in the same magnetic configuration as in the above. In the Hall MHD equations, the Ohm's law $\boldsymbol{E} = -\boldsymbol{u} \times \boldsymbol{B} + \eta \boldsymbol{J}$ is replaced by $\boldsymbol{E} = -(\boldsymbol{u} - \varepsilon \boldsymbol{J}) \times \boldsymbol{B} + \eta \boldsymbol{J}$, where $\boldsymbol{u}$ and $\boldsymbol{J} = \nabla \times \boldsymbol{B}$ are the vectors of the velocity and the current density, respectively. An advantage of adopting the Hall MHD model is that the initial MHD equilibrium is an equilibrium of the Hall MHD model, too, in the ideal limit (that is, null dissipative coefficients). Consequently, it can give a good starting point to an extended MHD study, even though some other terms comparable to the Hall term are omitted from the equations. We do not expect the Hall term to suppress the ballooning modes solely by itself, but aim to clarify roles of the Hall term and provide basic information to carry out further extended simulations.

In Fig.3, the time evolution of the Fourier energies (that is the amplitude squared and integrated in the radial direction ψ) of the parallel velocity component are shown for both the Hall MHD and MHD simulations with the same dissipative coefficients ($\eta = \mu = \kappa_\perp = 1 \times 10^{-6}, \kappa_\parallel = 1 \times 10^{-2}$). The Hall term is set as $\varepsilon = 0.05$. The time series of $0 \leq m \leq 9$ Fourier energies are plotted in Figs.3(a)($n = 0$) and (c)($n = 1$). The growth of the Fourier energies in the MHD simulation are also shown in Figs.3(b) and (d) the comparison with (a) and (c), respectively. The $n = 0$ Fourier energies grow rapidly just in the beginning of the Hall MHD simulation (Fig.3(a)), while they stay relatively small in the MHD simulation (Fig.3(b)). The difference may be understood as follows. In the MHD equations, the magnetic field is driven by $\nabla \times (\boldsymbol{u} \times \boldsymbol{B})$, and the induction is initially small because of the small $\boldsymbol{u}$. In the Hall MHD simulation, the induction equation is governed by $\nabla \times [(\boldsymbol{u} - \varepsilon \boldsymbol{J}) \times \boldsymbol{B}]$. The Hall term does not work while the force balance $\nabla P = \boldsymbol{J} \times \boldsymbol{B}$ is kept perfectly because $\nabla \times (\varepsilon \boldsymbol{J} \times \boldsymbol{B}) = \nabla \times (\varepsilon \nabla P) = 0$. However, the Hall term can become large once the magnetic field is perturbed because the fluctuation component of the current can be larger than the velocity fluctuation in the initial perturbed field. Once the magnetic field is perturbed, the parallel heat conduction works to smooth the pressure field along the perturbed magnetic field lines and cause a tentative and a large imbalance between ∇P and $\boldsymbol{J} \times \boldsymbol{B}$. We consider that the intrinsic nonlinearity of the parallel heat conduction,

$\nabla\cdot\left[\kappa_{\|}(\nabla_{\|}P)\right]=\nabla\cdot\left[\kappa_{\|}(\boldsymbol{e}_b\cdot\nabla P)\right]=\nabla\cdot\left[\kappa_{\|}\left((\boldsymbol{B}\cdot\nabla P)/|\boldsymbol{B}|\right)\right]$, which doe not necessarily suppress a perturbation but can perturb the equilibrium stronger, appear cooperatively with the Hall term in this simulation. As the consequence, some $n=0$ energies of the parallel flow are generated rapidly. In contrast to the $n=0$ energies, the $n=1$ Fourier energies in the Hall MHD simulations grow almost exponentially (Fig.3(c)). The growth of energies of $m/n=2/1$ (the main Fourier coefficient of the $n=1$ mode) and a few other Fourier coefficients (side-bands of the mode) in Fig.3(c) is brought about by the ballooning instability, as we can see in their MHD counterparts in Fig.3(d). However, other $n=1$ energies such as $m=5$,6,7 and so on grow because of the nonlinear couplings of the unstable Fourier coefficients with the $n=0$ coefficients in Fig.3(a). The $n=0$ energies in Fig.3(a) reach a finite-amplitude state before the linear modes begin to grow at $t\simeq 60\tau_A$ where τ_A is the toroidal Alfén unit. (Hereafter, we assume the time unit τ_A in this article, and the symbol is omitted.) Then couplings of the $n=0$ coefficients with the unstable $n=1$ coefficients such as $m/n=1/1$ and $2/1$ cause growth of the non-resonant Fourier coefficients ($m/n=5/1$, $6/1$ and so on) with the same growth rates as that of the $m/n=2/1$ energies. The time evolution of the energies of the $n\geq 2$ energies are essentially mixtures of the non-resonant growth associated with the rapid growth associated with the moderate $\kappa_{\|}$ and the growth of linearly unstable modes. (Figures are omitted.) These observations show that the Hall term and the parallel heat conduction work cooperatively to generate parallel flow and enhance nonlinear couplings in the time evolution.

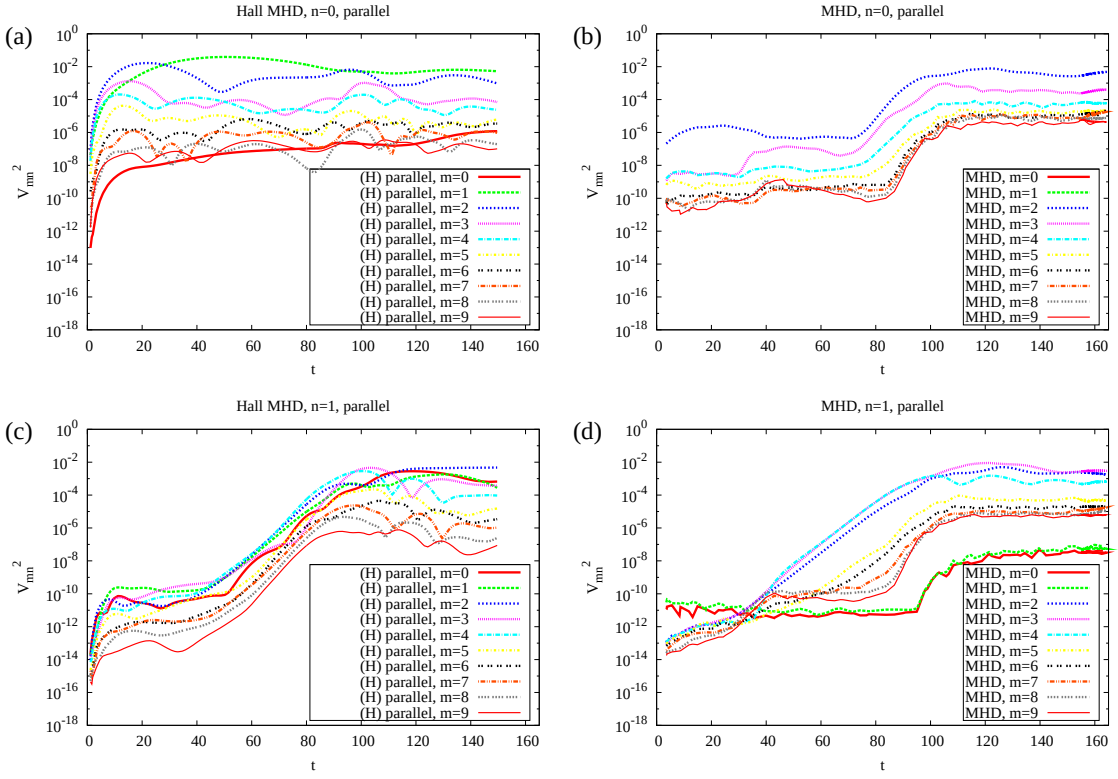

FIG. 3: Time evolutions of the Fourier energies in the Hall MHD and the single-fluid MHD simulations.(a)$n=0$(Hall MHD), (b)$n=0$(MHD), (c)$n=1$(Hall MHD), and (d)$n=1$(MHD) energies.

In Fig.4, we plot the mean pressure profile P_{00} of the Hall MHD simulation. The beta value in the saturated pressure profile ($t=135$) of the Hall MHD simulation is lower than that in the MHD simulation in Fig.2. The reduction of the beta value should be attributed to the strong velocity generation which we have seen in Fig.3. It suggests that the existence of the Hall term does not necessarily improve the saturated pressure profile, at least when the moderate $\kappa_{\|}$ is adopted.

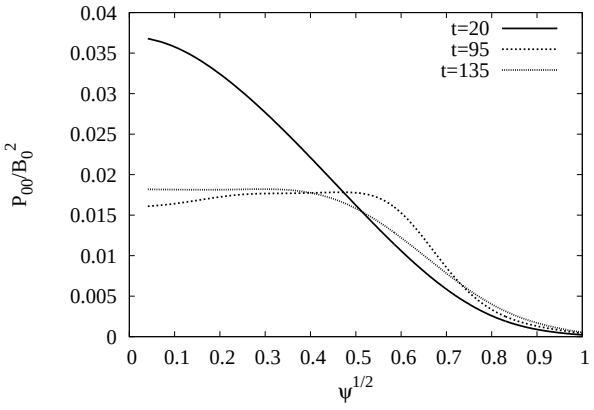

FIG. 4: The mean pressure profile in the Hall MHD simulation.

5 Effects of sub-grid-scales

As we have mentioned in §.2, we do not necessarily expect a stabilization of the ballooning modes solely by the Hall effect because such a stabilization effect often depends on the detailed plasma profile. Furthermore, since the moderate $\kappa_{\|}$ causes a large difference from an ideal stability analysis, the stabilization by the Hall term in the sense of an ideal MHD system is less expected. We rather intend to study basic natures of the Hall term in the growth of unstable modes. For this purpose, we compare two Hall MHD simulations with the same parameter but the different grid numbers, (H)$193\times193\times640$ and (L) $97\times97\times640$. In the latter run, the coarsest grid width in the real space and the ion skin depth is comparable to each other. The high resolution run (H) resolves the ion skin depth scale reasonably while the low resolution run (L) does not necessarily resolves it. In Fig.5, the time evolutions of the energies of the main Fourier coefficients of (a)$n=1$,(b)2,(c)3 and (d)4 unstable modes are compared between the two runs. Although the time evolutions in the two runs are qualitatively similar to each other, the some Fourier energies are almost 100 times different. (See for example, the $m/n=4/2$ coefficient of the normal and binormal velocity components, and the $m/n=5/3$ coefficient of the parallel velocity component between the two runs.) By investigating time evolutions of many Fourier energies we find that the low-resolution simulation underestimate the energies over many wave numbers in comparison to the high-resolution simulation.

We can understand these numerical results as follows. Since the low-n Fourier coefficients are well resolved even with the smaller number of grid points $97\times97\times640$, it is difficult to attribute the underestimate of the Fourier energies to a numerical viscosity associated with the limited numerical resolution. We should rather attribute the difference to the Hall term. It is conjectured that the Hall term causes the energy transfer from the scales around the ion skin depth to the larger scales, that is an inverse energy transfer in the wave number space. Since the ion skin depth is not sufficiently resolved, the inverse energy transfer is not well expressed, and the large scales of the magnetic field are not enhanced by the inverse transfer sufficiently. The consequence is that the $\boldsymbol{J}\times\boldsymbol{B}$ term in the momentum equation term does not enhance the flow field sufficiently. This understanding is consistent with numerical results on the homogeneous Hall MHD turbulence simulation, in which the Hall term causes the energy transfer from the scales around the ion skin depth to both the lower and higher scales[15]. Although the 3D Hall MHD simulation in LHD and the homogeneous Hall MHD turbulence are different to each other in many aspect, a comparison between them can make a sense because the plasma flows and magnetic field fluctuations in the

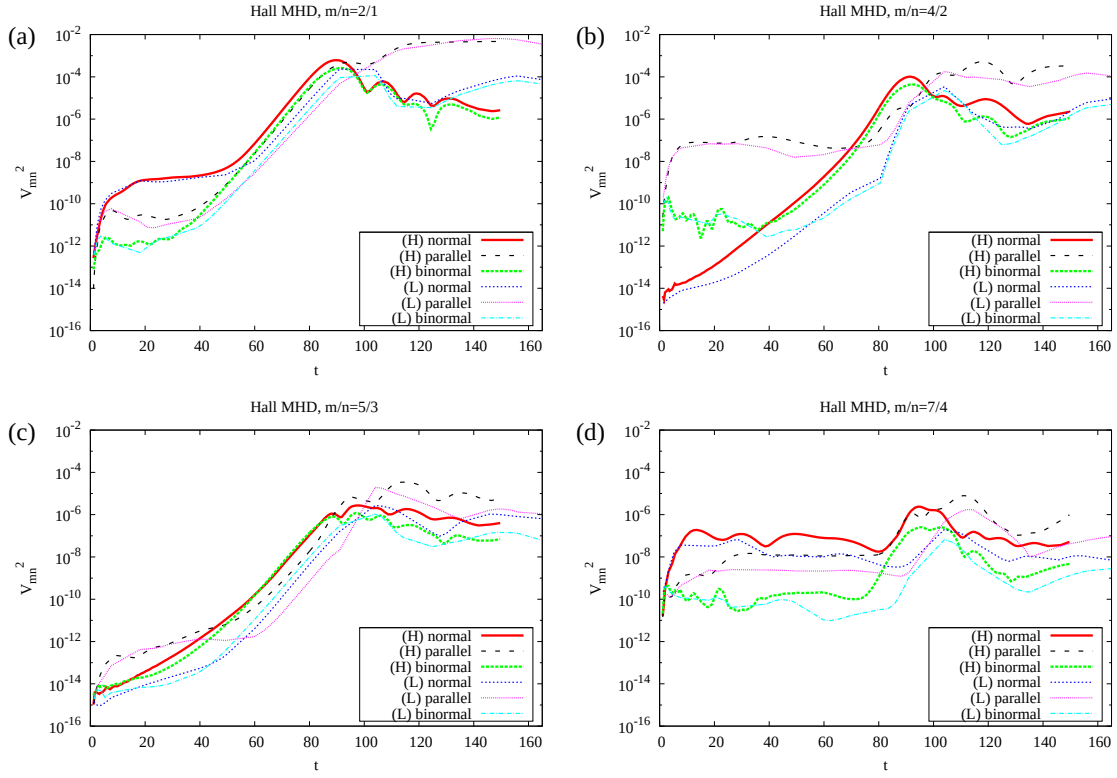

FIG. 5: A comparison of Fourier-energy evolutions between the two Hall MHD simulations.

LHD simulations are fully developed and behave turbulent as the consequence of the enhanced nonlinear couplings in §4. The study in the homogeneous turbulence suggests that the sub-grid-scales can be modeled as to cause the inverse energy transfer when the grid width (or filter width of a large eddy simulation) is comparable to the ion skin depth, or can be modeled by a typical eddy/current diffusivity when the grid with or the filter width is quite smaller than the ion skin depth.

6 Concluding Remarks

We study the Hall MHD dynamics from a fairly unstable MHD equilibrium of the LHD, as the first step to extend our study to extended MHD simulations. Our Hall MHD simulations show that the time evolution of the Hall MHD system can be governed not only by the growth of the unstable ballooning modes but also by the rapid generation of the parallel flow due to the cooperative work of the Hall term and the moderate $\kappa_{\|}$. In such a case, the stabilization mechanism of the Hall term does not necessarily improve the saturated pressure profile. We also study sub-grid-scale effects of the Hall MHD term. In our study, the Hall term works to cause the inverse energy transfer from the scales around the ion skin depth to the larger scales. According to the numerical results of the homogeneous Hall MHD turbulence, we might be able to model the sub-grid-scale of the Hall term by a typical eddy/current diffusivity when the numerical simulation well resolves the ion skin depth scale. Such a modeling will be required to carry out extended MHD simulations quickly.

Numerical simulations in this article are carried out in the NEC SX-8 “LHD numerical analysis system”, and the HITACHI SR16000 “Plasma Simulator” of the National Institute for Fusion Science (NIFS), Japan. The authors would like to thank members of the Numerical Experiment

Project in NIFS for fruitful discussions. This research was partially supported by the NIFS collaborative Research Program (NIFS09KNXN154,NIFS10KDAS002, NIFS10KTAS001)

References

[1] MOTOJIMA, O., et al., "Initial physics achievements of large helical device experiments", Phys. Plasmas **6** (1999) 1843-1850.

[2] MOTOJIMA, O., et al., "Overview of confinement and MHD stability in the Large Helical Device", Nuclear Fusion **45** (2005) S255-S265.

[3] SAKAKIBARA, S., et al., "MHD characteristics in the high beta regime of the Large Helical Device", Nuclear Fusion **41** (2001) 1177-1183.

[4] WATANABE, K., et. al., "Progress of High-Beta Experiments in Stellarator/Heliotron", Fusion Sci. Technology **46** (2004) pp.24–33.

[5] WATANABE, K., et. al., "Effects of global MHD instability on operational high beta-regime in LHD ", Nucl. Fusion **45** (2005) 1247-1254.

[6] MIURA, H., et al., "Nonlinear MHD Simulations in the Large Helical Device", Phys. Plasmas **8** (2001) 4870.

[7] MIURA, H., et al., "Non-disruptive MHD Dynamics in Inward-shifted LHD Configurations", 20th IAEA Fusion Energy Conference (2004), IAEA-CSP-25/CD/TH/2-3.

[8] MIURA, H. et al., "Direct Numerical Simulation of Nonlinear Evolution of MHD Instability in LHD", AIP Conference Proceedings **871** (2006) pp.157-168.

[9] MIURA, H. et al., "Nonlinear Evolution of MHD Instability in LHD", Fusion Science and Technology **51** (2007) pp.8-19.

[10] NAKAJIMA, N., et al., "Growth Rates and Structures of MHD Modes in Stellarator/Heliotron", J. Plasma Fusion and Res. SER. **6** Vol.6 (2004) 45-50.

[11] MIURA, H. et al., "Influences of Moderate Wavenumber Ballooning Modes", Nuclear Fusion **50** (2010) .

[12] HARAFUJI, H., et al., "Computational Study of Three-Dimensional Magnetohydrodynamic Equilibria in Toroidal Helical Systems", J. Comp. Phys., **81** (1989) 169.

[13] SAKAKIBARA, S., et al., "Effects of Resonant Magnetic Fluctuations on Plasma Confinement in Current Carrying high-β Plasmas of LHD", Plasma Fusion and Res. **1** (2006) 003.

[14] HUBA, J.D., "Finite Larmor radius magnetohydrodynamics in the Rayleigh-Taylor instability", Phys. Plasmas **3** (1996) pp.2523-2532

[15] MIURA, H., "Influences of short-wave truncation to spectral energy budget in Hall MHD turbulence", to appear in Plasma and Fusion Research (2010) .